Bulletin of Earth Sciences of Thailand

3D Facies Modeling of Mangahewa C Sand in Maui B Gas Field, Taranaki Basin, Offshore New Zealand

Anh Huyen Nguyen*

Petroleum Geoscience Program, Department of Geology, Faculty of Science,
Chulalongkorn University, Bangkok 10330, Thailand
*Corresponding author email: anhnh01pvu@gmail.com

Abstract

Building a reservoir model for volumetric calculation is often done based on a single geological concept which is expected to represent the true geological picture. This approach might not capture the full range of uncertainties related to the complexities of geology. The objective of this study is to build an alternative model based on a separate geological concept from the one that is the most likely case and then to compare the net rock volume calculation of these models to see the impact on the final results. The depositional environment was interpreted based on a combination of paleogeography maps, well logs, seismic attributes and core description in Maui B field, Taranaki Basin, offshore New Zealand. The facies models contain eight depositional facies broken down into three groups, namely marginal marine, shallow marine and shelf. The first model has the main reservoir interpreted as upper shoreface sand while the second model assumes that the sand has been deposited in tidal channel systems. The modeling uses Petrel software package which combines object-based and pixel-based modeling termed Sequential Indicator Simulation (SIS) to generate an output. The SIS algorithm was applied to define the background and then objects such as channels and tidal mouth bars were introduced to the previously defined background. The results indicated there is a 42.8% difference in net rock volume between the two models corresponding to 33.2 Bcf of net rock volume or 340 Bcf of gas recoverable reserves. This suggests the geological concept has a great effect on the final volumetric estimation and an alternative model should be constructed in order to capture the range of uncertainties related to net rock volume calculation.

Keywords: Maui B Gas Field, 3D Facies Modeling, Sequential Indicator Simulation, Object-based Modeling, Depositional Environment

1. Introduction

Maui B is a mature gas-condensate field located within the Taranaki Basin in the west offshore part of North Island, New Zealand (Figure 1). Estimated recoverable reserves are around 3.83 Tcf (University of Canterbury Campus, 2006). With cumulative production of 3757 Bcf (Ministry of Business, Innovation and Employment, New Zealand, 2017), Maui field has reached depletion stage where production drops after 38 years. The middle Eocene C sand contains the majority of the gas-condensate reserves in the Maui field.

The Taranaki Basin has had a complex history from the Late Cretaceous through to the Neogene, encompassing rifting, passive subsidence and compressional tectonics related to the evolution of the Australia-Pacific plate boundary, and late back-arc rift phases (Strogen et al., 2012). Development of rifting was the result of extensional stresses during the breakup of Gondwanaland. The basin later underwent fore-arc and intra-arc basin development, due to the subduction of the Pacific Plate under the Australian Plate at the Hikurangi Subduction System (Walcott, 1987).

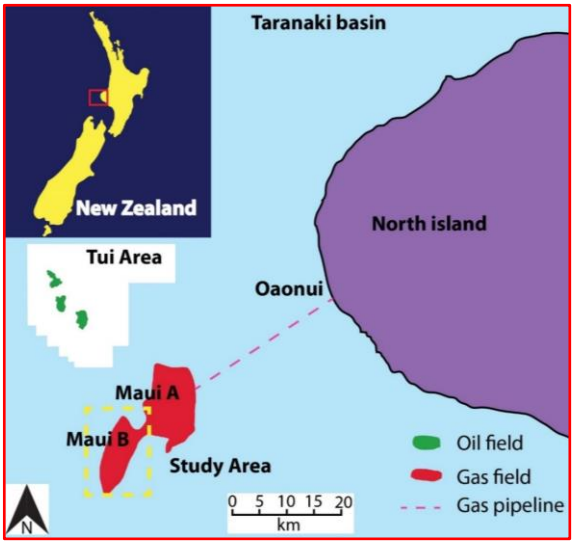

Figure 1. Study area located in offshore Taranaki Basin, 35 km offshore from the North Island (Modified after AWE, 2015)

The aim of this study is to build a representative model for a realistic stratigraphic understanding of the Magahewa C sand. Based on multiple realistic depositional models, prediction of sand body distribution as well as volumetric calculation, such as gross rock volume (GRV) and net rock volume (NRV), can be made. This study will focus on identifying alternative possibilities of depositional environments to account for geological uncertainties which should be considered in order to avoid drilling dry holes in the development phase. Separate reservoir models will be constructed based on different possible reservoir depositional environments to show the impact on net rock volume for different reservoir models.

2. Methodology

Sequential Indicator Simulation (SIS) which is a variogram-based method was utilized in this study. This method is a benchmark in geocellular modeling and has been recognized as a reasonable approach when there are no well-defined geometries that could be incorporated into object-based modeling (Deutsch, 2006). SIS builds on the underlying geostatistical method of kriging, but then introduces heterogeneity using a sequential stochastic method to draw Gaussian realizations using an indicator transform. The indicator is used to transform a continuous distribution to a discrete distribution (Ringrose and Bentley, 2015). The process begins with generating a random path to visit each grid node and a facies code will be assigned by calculating the probability of each facies being present at the current cell.

Object-based modeling algorithm is also incorporated into the workflow to model facies with discrete shape in 3D space for which another model element has been defined as the background. For example, tidal channel sands are distributed in previously defined intertidal region.

3. Modeling workflow

The workflow begins with data screening and analysis. The seismic interpretation is then carried out to build a structural model which is later converted to a 3D structural grid to set a framework for the models. Electrofacies, seismic attributes and paleogeography maps are the main sources for constructing conceptual models which are mainly based on the depositional environment interpretation. After preparing all geomodel elements with high confidence, variogram analysis will be performed to populate hard data at the wellbores into 3D space. The output is then assigned as a background for objects generated from an object-based modeling algorithm. Finally, petrophysical properties derived from well logs are assigned to each facies to calculate gross rock volume, net rock volume and hydrocarbon volume. Normally a single depositional model is used. However, the aim of this study is to calculate the effects of using different depositional models.

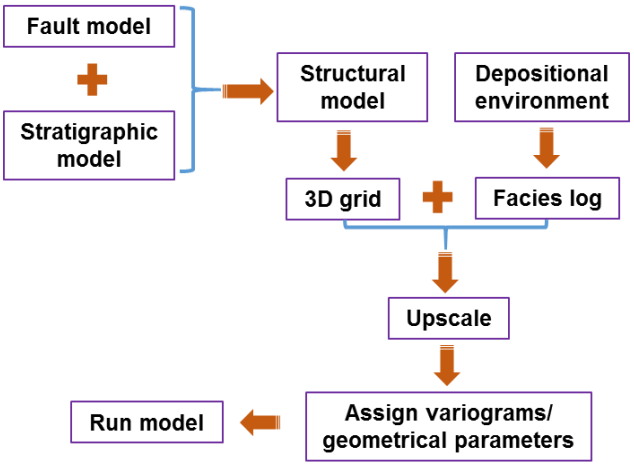

Figure 2. Geomodeling workflow applied in this study

4. Interpretation

4.1 Seismic Interpretation

Synthetic seismograms were modeled from 3 wells: Maui-1, MB-P8 and MB-Z11 after correcting sonic and density curves. The seismic data have negative polarity so the wavelet extracted from seismic cube (2-3 seconds) was rotated 180^{o} which means the resulting synthetic also has negative polarity. Reference traces were generated by splicing along the boreholes and compared to the synthetic.

There are two main reverse faults in Maui B area trending in NNE-SSW direction. The major fault called Whitiki controls the orientation of structural trap. The faults propagate from basement and possibly penetrate to a much shallower part though obvious displacements cannot be observed due to limitation of seismic resolution. For horizon mapping, the three most important events called top C1, top C2 and base C2 were picked. They fall into peak events with strong reflectivity because the gas sand has a low acoustic impedance compared to shale at reservoir depth. The next step is to convert these horizons to surfaces and then smooth them out using Petrel software (Figure 3). These surfaces were then used to build a 3D grid that constrains facies distribution. Water bottom, top and base of Tikorangi Limestone were also mapped in order to build a velocity model for time-to-depth conversion purpose.

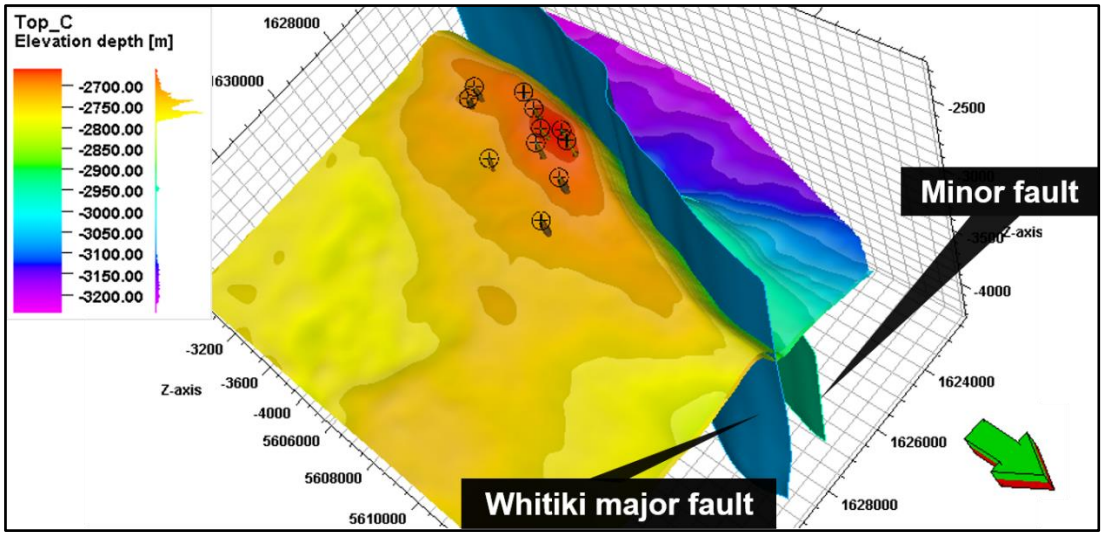

Figure 3. Depth-converted faults and surfaces. All wells are located around a structural high

As can be seen from the depth structure map, the main trap is placed against the main reverse fault – the Whitiki fault. All wells are located around a structural high that holds hydrocarbons forming a fault controlled structural trap. The footwall of the Whitiki fault has little potential of a trapping mechanism although there are still chances of reservoir occurrence. This fault acts as a compartment that limits net rock volume calculation to the potential east side (hanging wall) and not on the non-potential west side (footwall).

4.2 Petrophysical Interpretation

The presence of gases in the formation affects density and neutron porosity reading by lowering their values and forming negative crossover between these curves. There are some thin intervals that have bulk density greater than 2.65 g/cm3 and neutron porosity smaller than 0.12 v/v (Figure 4) which can be due to carbonate cementation in the pore space. The four most important properties that were generated are clay volume, porosity, water saturation and net-to-gross (Figure 5).

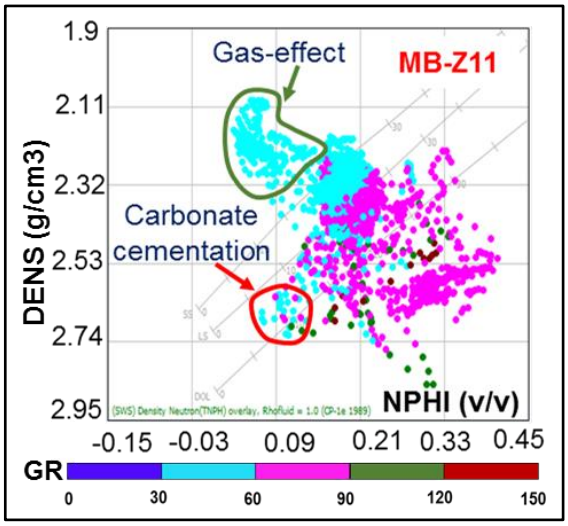

Figure 4. Neutron-Density crossplot in MB-Z11. Gas-effect region is indicated by dark green circle and carbonate cementation is highlighted by red circle

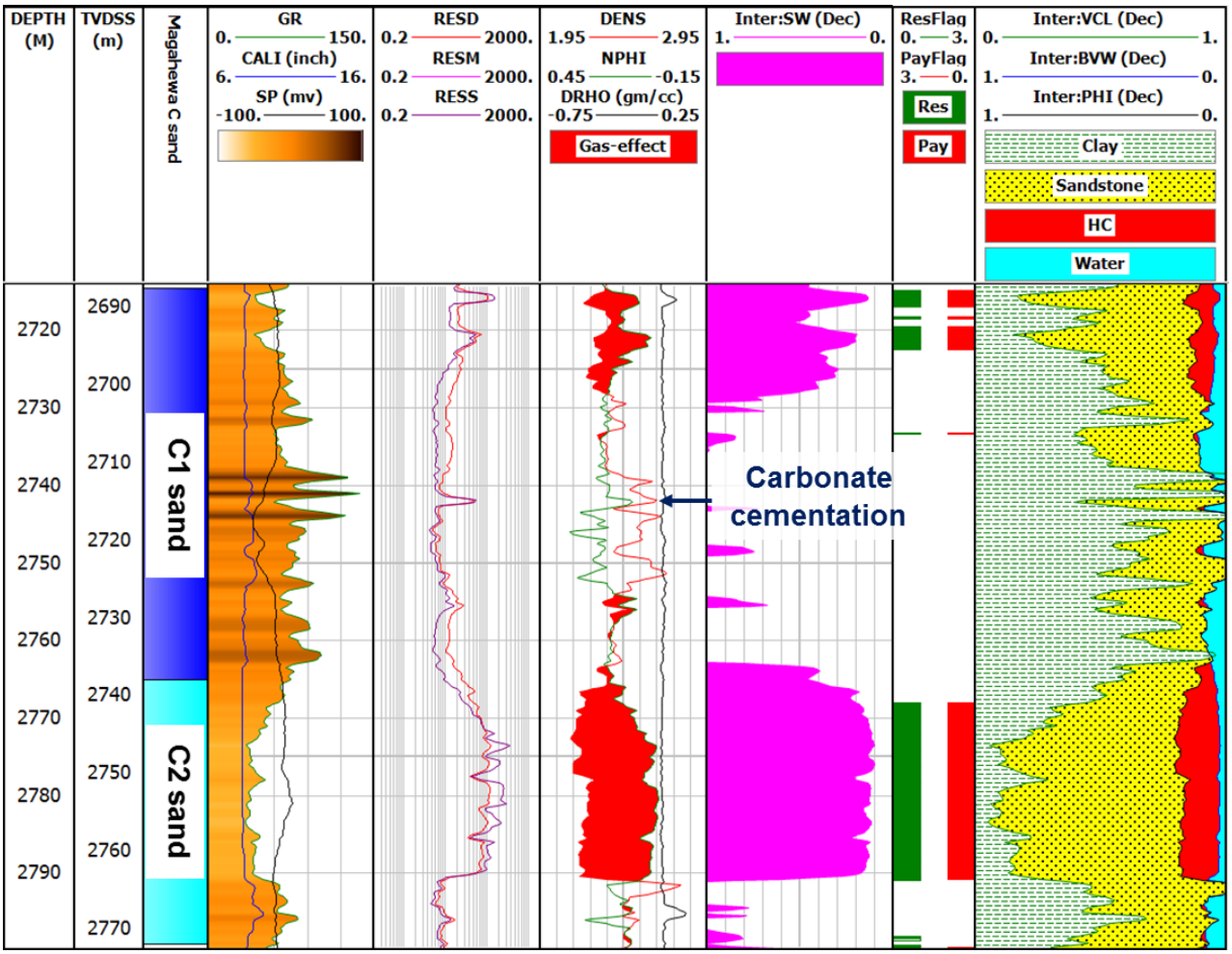

Figure 5. Petrophysical interpretation in Maui 7. Intervals of pay sand are highlighted in track No.7 by "Pay" (red); "Res" (green) represents net reservoir

The overall results have shown that the lower sand (C2 sand) contains higher quality reservoir than the upper one (C1 sand). Firstly, clay contents make up 10-15% in C2 sand while that value for reservoir in C1 is around 20-40%. Secondly, thicker reservoir interval of about 20-30 m is found in C2 sand as compared to C1 sand with net reservoir of around 10 m. In terms of storage capacity, C1 sand which is partially saturated with hydrocarbon has 2-3% lower porosity than that of C2 sand (nearly fully-saturated). The average value for porosity of reservoir intervals is approximately 20%. These values will be input into volumetric calculation equation for each depositional facies.

4.3 Depositional Environment Interpretation

Paleogeography maps drawn by King and Thrasher (1996) from middle Eocene to late Eocene proposed that there was an overall transgression within Mangahewa Formation. Depositional strike was in NE-SW direction with the source of sediments from the Southeastern. Higg et al., (2012) recognized that the upper Eocene Magahewa Formation is a mixture of marginal to shallow marine environment. The formation is capped by offshore mud of Turi Formation. The lowest section of the C sand was deposited in coastal and lagoonal environments while the bulk of the overlying C sand was deposited as highstand, regressive shoreline sands that are partitioned by thin, tight transgressive deposits (Bryant, 1995).

In this study, various sources of data including core description in well Maui 7, seismic attributes, paleogeography maps and wireline logs have been integrated to reduce the uncertainty that is inherent to any reservoir geological model. There are eight identified

facies broken into three groups: shelfal mudstone, shallow marine and marginal marine environments.

Shelfal Mudstone

Shelfal mudstone is found in all wells drilled in Maui B region and on top of Mangahewa C sand with thickness of around 60-80 m. This facies acts as a regional seal over the entire Magahewa Formation. Moreover, it indicates possible transgression of the offshore facies to the landward direction. Apart from this thick shelfal mudstone covering the entire C sand, thinner layers of approximately 5-7 m of shelfal mudstone associated with maximum flooding surface were noticed within Magahewa C sand (Figure 6).

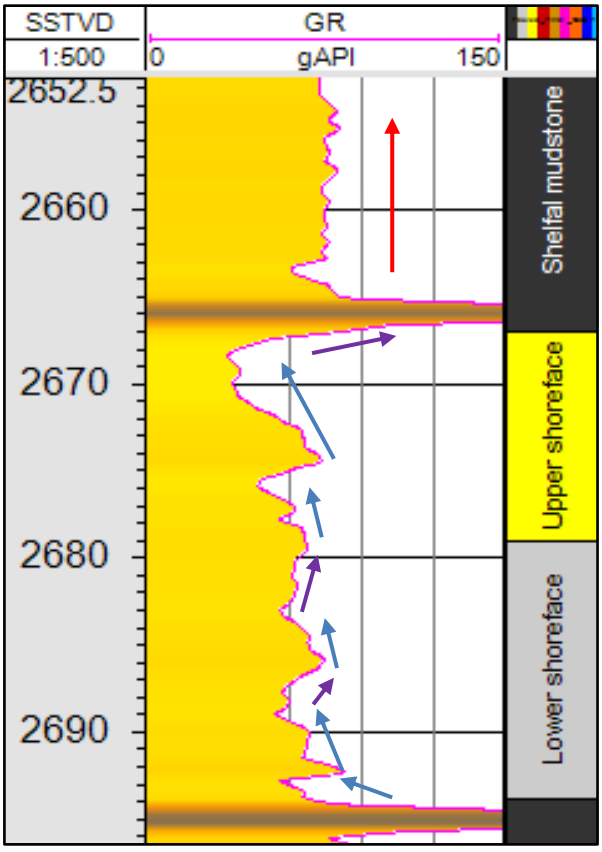

Figure 6. Shallow marine facies association and shelfal mudstone in MB-P8. An overall coarsening upward trend is observed

Shallow Marine Facies Association

Upper shoreface

According to core description from Maui 7, the interval from 2686 to 2696 mTVDSS contains fine to coarse sandstone and the upper most part is characterized as a fining-upward sequence. On wireline log, Gamma Ray (GR) values range from 30 to 60 API with a clear cleaning-upward sequence from 2668 to 2675 mTVDSS in MB-P8 (Figure 6). Upper shoreface sand thickness is around 5-15 m.

Sweetness attribute extraction of the top C1 and C2 sands are shown in Figure 7. This attribute is the product of amplitude divided by frequency. It can highlight region of gas-bearing sand which has low frequency and high amplitude. On C1 sweetness attribute map, a linear, SW-NE trending zone of high amplitudes is believed to be mainly related to good reservoir area associated with the distribution of shoreface sands. These sands pinch out seaward toward the northwest. The dimming of amplitudes to the S-SW most likely reflects the landward pinch-out of the shoreline sands although this may be partly obscured by tuning effects associated with the gas-water contact in the Maui B area.

In terms of reservoir geometry, upper shoreface systems produce sheet sand body, aligned subparallel to paleo-shoreline. These sand bodies are the best reservoir because they are laterally extensive, possibly up to 100 km across Maui field and the sands are clean, well-sorted formed during upper flow regime (Reading, 1996).

Lower shoreface

This depositional environment is separated from upper shoreface by fair-weather wave base. GR values of lower shoreface sand is higher than that of upper shoreface sand, at around 60-90 API. On core, the interval from 2696 to 2710 is dominant by fine sandstone with occasional burrow and shaly partings. Lower shoreface reservoir has higher mud contents, mostly heterolithics making it difficult to detect on well logs since the sand thickness is below conventional log resolution. These heterolithics create small-scale heterogeneities and act as vertical flow barrier.

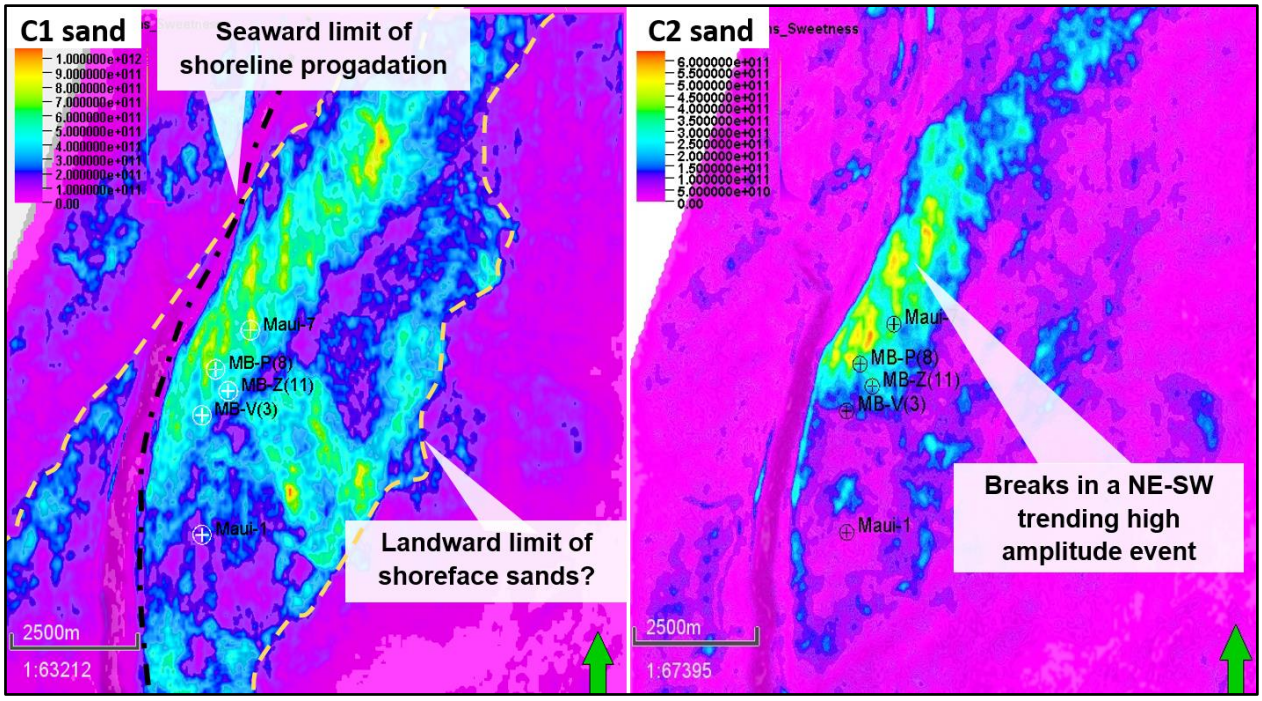

Figure 7. Sweetness attribute extracted below top C1 and C2 sand surface with 20 ms TWT window. High amplitude (red to yellow) regions are associated with sands; Low amplitudes are associated with shales (purple to pink)

Marginal Marine Facies Association

Tidal channel fill/tidal point bar

Grain size decreases upward corresponding to an increase in GR value in well MB-Z11 (Figure 8). This is interpreted to be tidal point bars due to higher mud contents toward the top. The tidal channel fill facies has different point bar sands which might not be in connection compared to sands deposited in upper shoreface environment. Unfortunately, identification of these two depositional environments based on electrofacies can be challenging. For that reason, two separated models will be built assuming these clean sands are either upper shoreface or tidal channel fill so that the impact of different conceptual models on the output net rock volumes can be quantified.

Tidal mouth bar

The formation of this facies is a complex phenomenon, owing to the interactions of several processes such as wave and tides. GR responses in MB-W2 show a coarsening-upward trend with a funnel shape indicating progradation in sediment supply (Figure 9). The thickness of the tidal mouth bars interpreted from wireline logs is from 5 to 10 m.

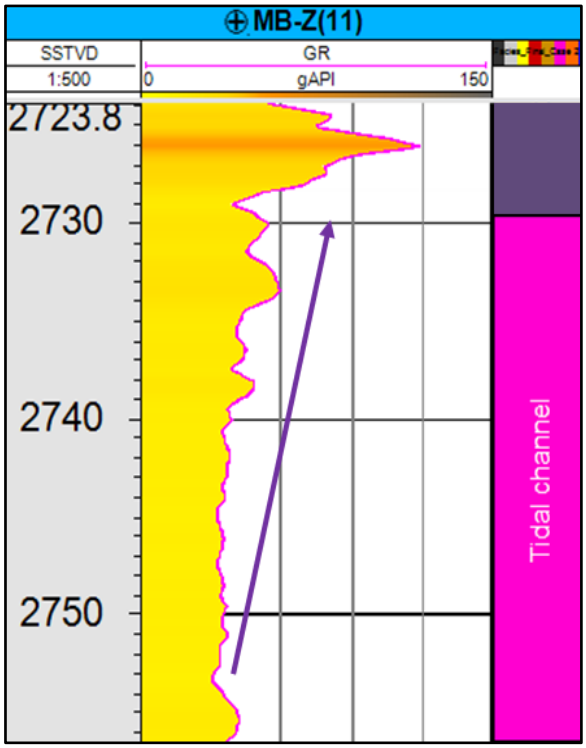

Figure 8. Tidal channel sand with fining upward trend

Tidal flats

Tidal flats are intertidal, soft sediment deposits which are normally found above water

at low tide and under water at high tide. In Maui-B field, tidal flat has an aggrading characteristic and relatively high GR response of around 60-80 API (Figure 9). Tidal flat interpreted on well logs is around 5m in thickness and is thinner as compared to other facies.

Estuarine

Estuaries are formed mainly by rising sea levels where accommodation space exceeds sediments supply and are often associated with transgressive system tracts. On well logs, estuarine channel sand is characterized by blocky, aggrading and low API GR response. These patterns indicate inter-bedded shale and sand. The thickness of estuarine channel sand can be up to 20 m (Figure 9).

Lagoonal mudstone

A lagoon is a shallow body of water separated from a larger body of water by barrier islands or reefs. This depositional environment mostly produces mud-dominated sedimentary rocks.

In Maui 7, the interval from 2718 to 2735 mTVDSS appears to have occasional burrows in fine sandstone and some thin siltstone beds toward the top. GR value is very high (>75 API) with an aggradational shape (Figure 9). Lagoonal mudstone can have thickness up to 25 m in the study area.

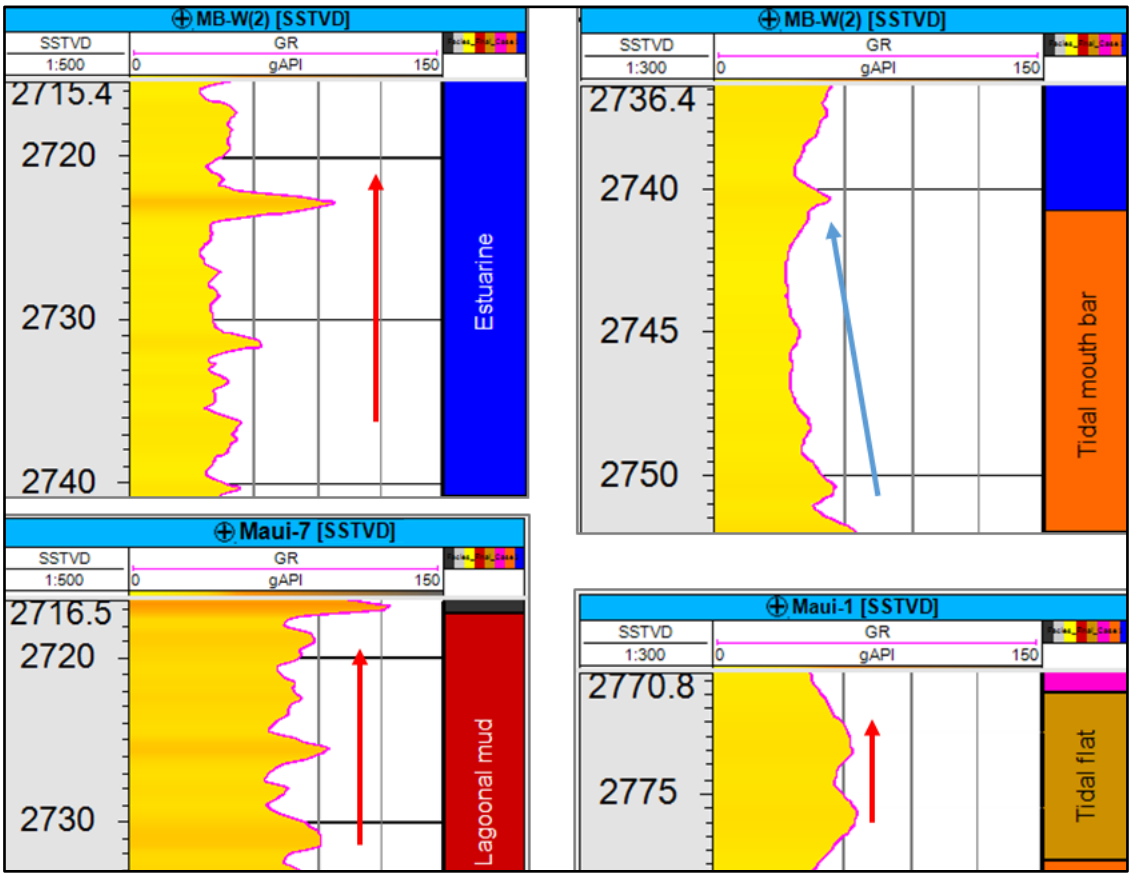

Figure 9. Marginal marine facies association. Estuary, tidal flat and lagoon show aggradation while tidal mouth bar has coarsening upward trend

5. Geological Modeling

5.1 Well Correlation

Correlation of thin shales and carbonate-cemented deposits associated with flooding surfaces was done first to establish a chronostratigraphic framework, followed by subdividing the sand units between these markers. This approach has a benefit of avoiding correlating rock layers that were deposited at different geological time and therefore making more accurate prediction of reservoir behavior during the development phase. Seven key

flooding surfaces were identified, two of them are possibly associated with maximum flooding surfaces where there is presence of peaks in GR response.

Two models were built based on two possible depositional settings although there could be more models that were not tested in this study. Model #1 has C2 interpreted as upper shoreface sands which means the sands have good connectivity along depositional strike. In model #2, C2 sand is believed to be tidal channel sands. These sands are not in connection to each other as they are in the model #1 (Figure 10). Sweetness map extracted below top C2 sand with 20 ms TWT window (Figure 7) has shown that there is a NE-SW trending sand body although there are still breaks in the continuously high amplitude event. These observations advocate a higher chance of occurrence for model #1.

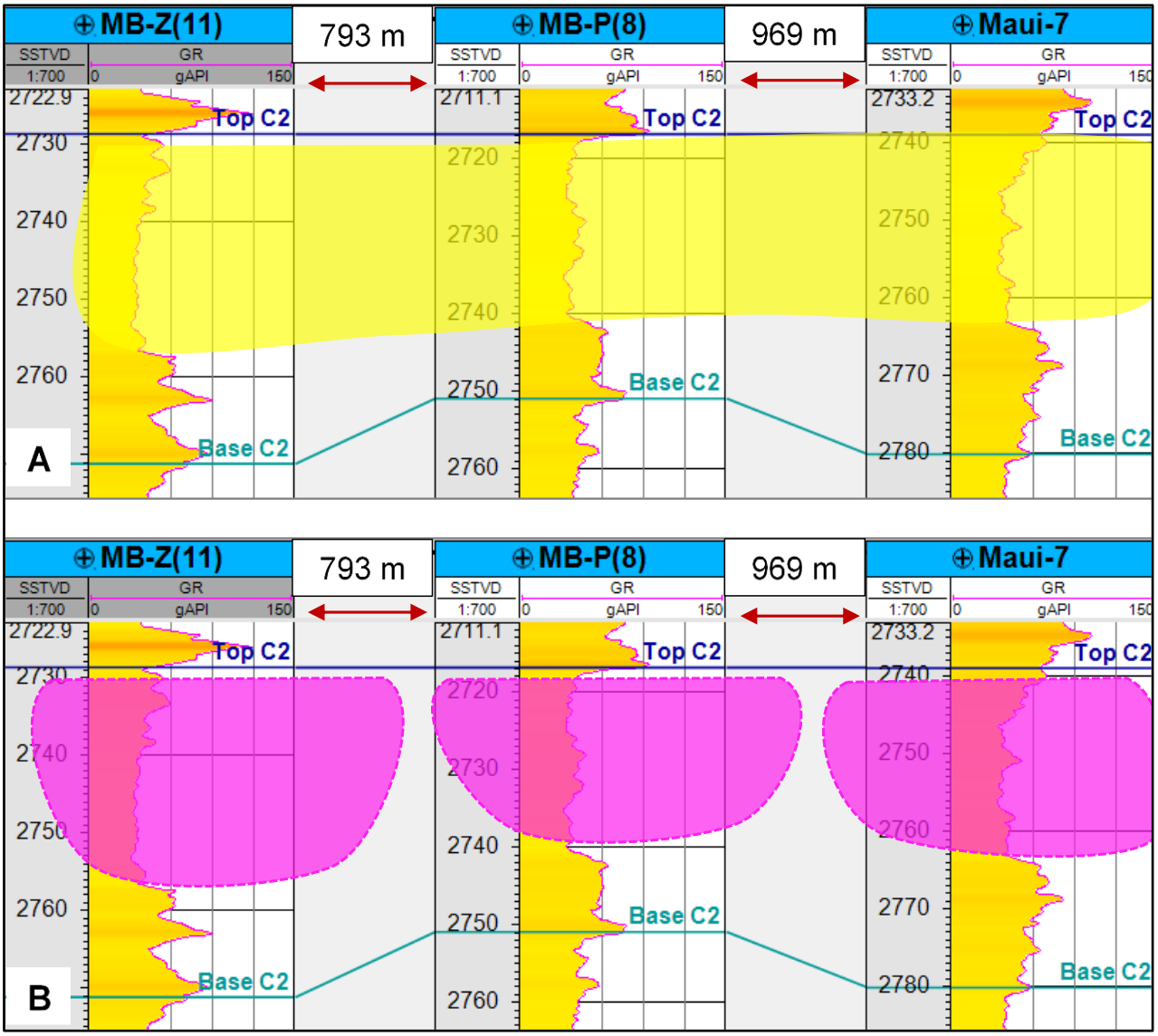

Figure 10. Two modeling concepts for C2 sand. The first model (A) has C2 sand interpreted as upper shoreface (yellow) while in the second one (B), thick gas sands are believed to be tidal channel sands (pink). With the well spacing of more than 790 m, these tidal channel sands are not in communication to each other and the opposite should be expected in case of upper shoreface sands

5.2 3D Gridding

There are several steps to build a 3D grid in Petrel software package (Figure 11). Fault modeling was done first to define fault geometry and reservoir structural control patterns. In this model, the main reverse fault which is Whitiki fault was used. Horizon modeling was then carried out to capture major boundary, including top C1/C2 and base C2. These horizons were adjusted to well markers during depth conversion. Next, well markers were utilized to capture reservoir level during zonation. Layering was later performed to specify reservoir property level, based on facies thickness and reservoir properties. The final step is to construct a 3D structural grid based on surfaces/faults that have been defined in the structural model. Since Maui B gas field is located on the east side of Whitiki fault, the west side was not included into the final 3D grid in order to avoid confusion during modeling process. The entire 3D grid contains 419958 cells: total 33 layers with average thickness of 3 m per layer and the grid dimension is 100x100 m, I x J x K = 101 x 126 x 33.

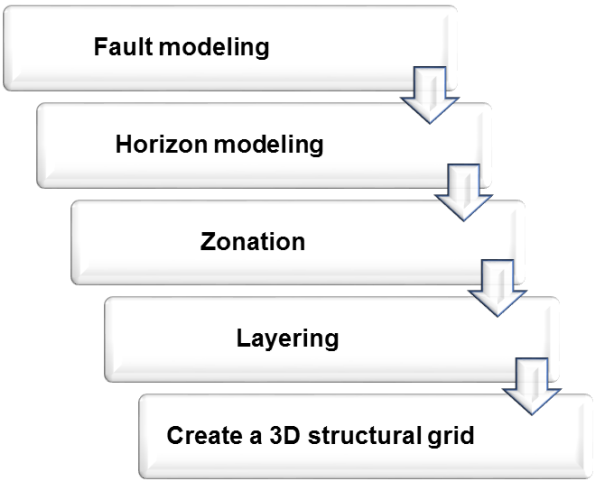

Figure 11. 3D gridding workflow in Petrel software package

5.3 Facies Modeling

Discrete facies log was upscaled to an existing grid. This process translates the higher resolution well log data to lower resolution grid cell values. The calculated result is an upscaled grid property that is only assigned to the 3D grid cells that are penetrated by the well trajectories. The facies log in all wells has been upscaled into 344 cells in the entire grid with "most of" method. This method selects the value which is most represented in the log for each particular cell and assigns it to the cell.

Illustration of the modeling process is shown in Figure 12. After modeling all facies (Shelfal mudstone, upper shoreface, lower shoreface, tidal flat, lagoonal mudstone, estuarine) using SIS method, objects were introduced into the model with the defined background of previously modeled facies. Tidal mouth bars were distributed in shallow marine (upper shoreface and lower shoreface) or in subtidal region while tidal channels were placed along with tidal flat in intertidal region.

6. Model Results

According to model statistics, the entire model #1 is made up mostly by tidal flat with 40.4% volume, followed by upper shoreface sand of around 24.2%. Facies with lowest proportion of 1.9% is estuarine, and tidal channel sand and tidal mouth bar facies account for 3.9% and 3.5%, respectively. In model #2, tidal channel sand facies has higher percentage of approximately 11.3% as compared to model #1. In contrast, only 6.9% of upper shoreface was found in model #2. This was expected when the models were designed.

As can be seen from cross-sections in Figure 14, tidal channel sands are not connected along depositional strike as they are just individual sand bodies. Shoreface sands have much better reservoir quality in terms of connectivity shown in Figure 13. In the two models for C sand, upper shoreface sands run across the whole Maui B field and contribute a large proportion of reservoir volume. The output models have met the initial design which accounts for the uncertainty related to depositional environment interpretation and they also honor well data.

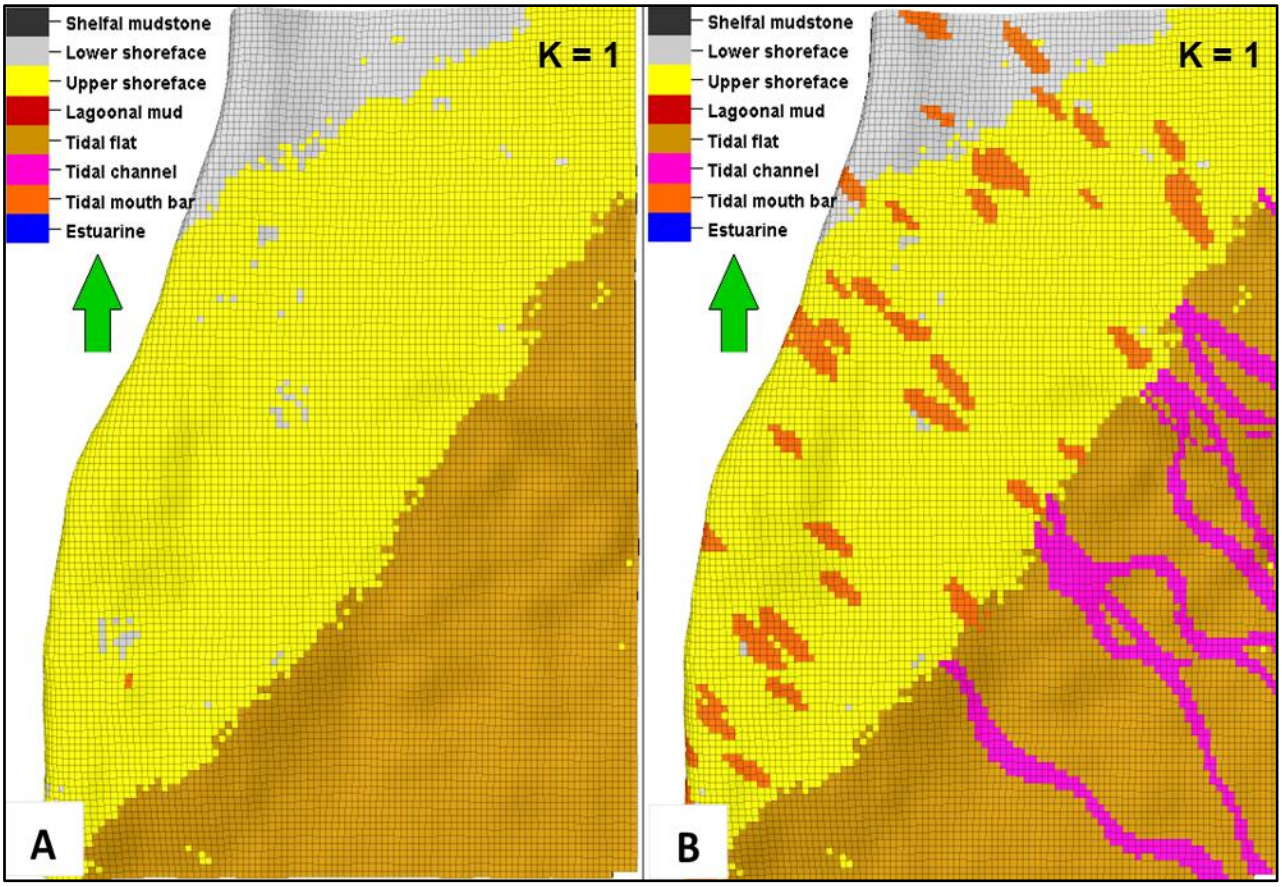

Figure 12. Facies model in C1 sand, model #2. A) Modeling facies using SIS algorithm to define background. B) Introducing objects (tidal channels/tidal mouth bars) into previously defined model

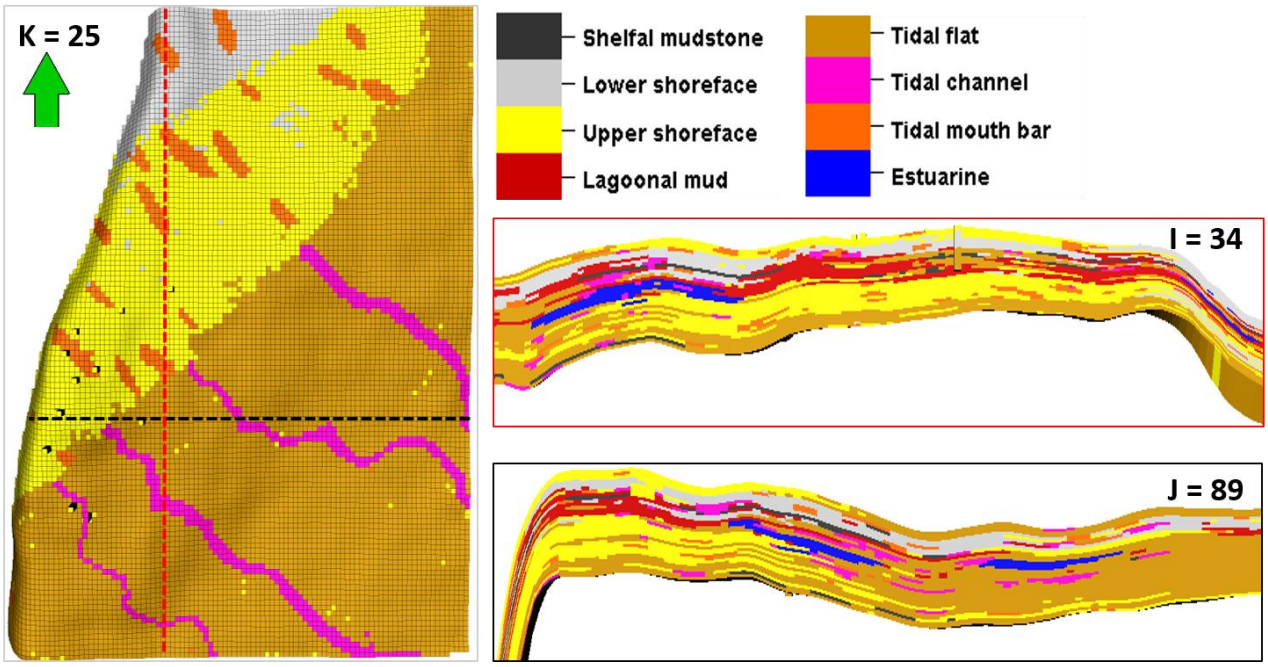

Figure 13. Final facies model #1. Yellow color represents upper shoreface sands which are continuous bodies along depositional strike in NE-SW direction

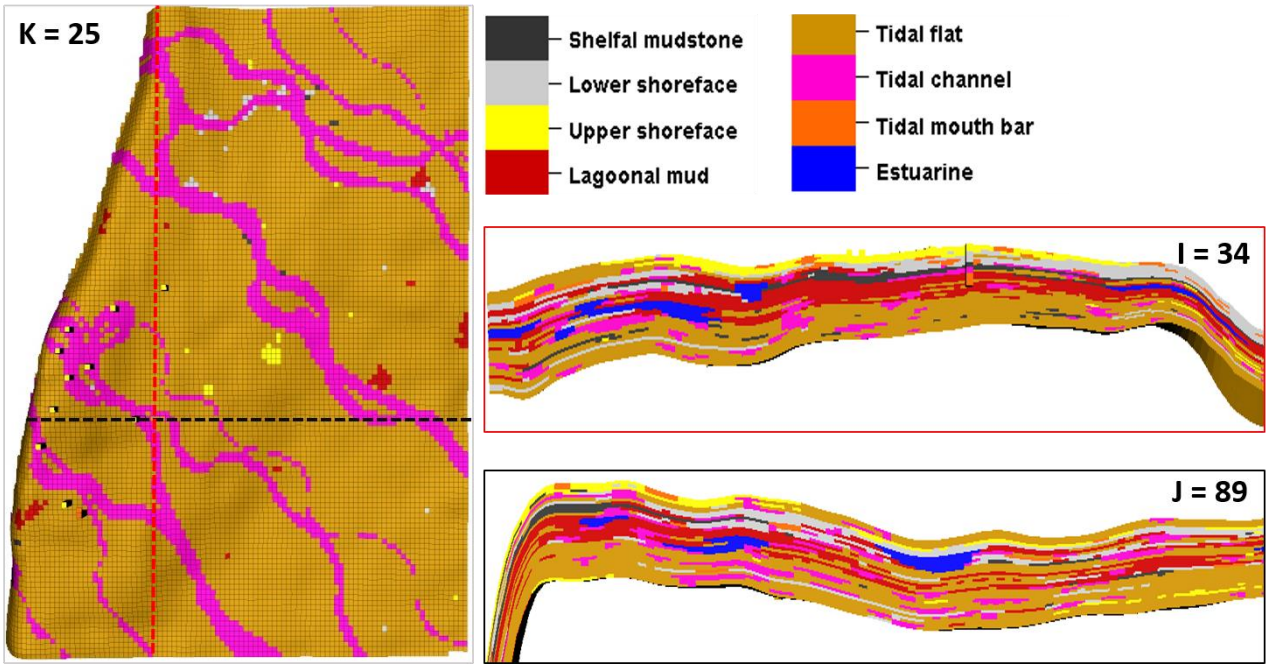

Figure 14. Final facies model #2. In the lower part, tidal channel sands (pink) are individual objects and are not always in connection

7. Net Rock Volume Calculation

Gas-water contact (GWC) can be seen on well logs in Maui 1 at around 2785 mTVDSS. The contact lies within the sandy interval and is the boundary between upper high resistivity, low water saturation zone and the lower part with low resistivity, high water saturation. The gross and net rock volumes were calculated above this datum. The total volume of the 3D grid is 389.5×10^9 ft^3 and 52% of the volume is located above GWC.

The results have shown that the gross rock volume is the same for two models, at around 5701.6 million m^3 (201.4 billion ft^3). However, there is a 42.8% difference of calculated net rock volume between the two models. More specifically, model #1 has net rock volume of around 2196.9 million m^3 (76.6 billion ft^3) and the number for model #2 is 940 million m^3 lower (33.2 billion ft^3). The difference is due to variation of facies proportions and their net-to-gross values. The volume difference represents around 340.4 Bcf recoverable gas.

8. Conclusions

- There is a 42.8% difference in net rock volume between the two models with separate geological concepts, leading to an additional 340.4 Bcf in gas reserves. This suggests geological concept has a great effect on the final volumetric estimation.
- Depositional environment of Mangahewa C sand in Maui B gas field is interpreted to be shallow marine and marginal marine with less dominant proportion of shelfal mudstone and there are eight facies associations to these depositional environments. In C2 sand, shoreface depositional environment is most likely to be the case with an alternative possibility of being tidal channel sands.
- For reservoir quality facies, upper shoreface sand is dominant in model #1 while tidal channel sand makes up a larger proportion than upper shoreface sand in model #2. That also means better reservoir connectivity is expected in model #1 since these shoreface sands are connected together along depositional strike.
- Combination of object modeling and SIS – a pixel-based modeling method has generated excellent outcomes that make more geological sense.

9. Recommendations

- Constructing alternative models with separate geological concepts is necessary in order to capture the uncertainties related to reserve estimation.
- Integration between various sources of data for interpreting depositional environment should be carried out to reduce uncertainties.
- In order to achieve desirable results, incorporation between object modeling and pixel-based modeling should be performed to build the rock models.
- Limitations of these algorithms should be well-understood before applying and a careful checkup of the results needs to be accomplished to avoid undesired outputs.

10. Acknowledgement

I would like to thank my supervisor Mr. Angus John Ferguson and my co-supervisor Dr. Piyaphong Chenrai, for their valuable advice and guidance at every stage of my graduate research. I greatly appreciate Schlumberger, IHS Global and Senergy for donating their interpretation tools. Finally, I am very grateful to the Petroleum Geoscience program for providing me scholarship to study at this distinguished program.

11. References

Bryant Ian D., Carl W.Greenstreet, and Walter R. Voggenreiter, 1995, Integrated 3-D Geological Modeling of the C1 Sands Reservoir, Maui Field, Offshore New Zealand, AAPG Bulletin, V. 79, No. 3, P. 351–374.

Deutsch Clayton V., 2006, A sequential indicator simulation program for categorical variables with point and block data: BlockSIS, Elsevier Computers and Geoscience 32, P.1669-1681.

Higgs K.E., King PR, Raine JI, Sykes R, Browne GH, Crouch EM, Baur JR, 2012, Sequence stratigraphy and controls on reservoir sandstone distribution in an Eocene marginal marine-coastal plain fairway, Taranaki Basin, New Zealand. Mar Pet Geol 32(1):110–137.

King P.R., and Thrasher G.P, 1996, Cretaceous-Cenozoic geology and petroleum systems of the Taranaki Basin, New Zealand, Institute of Geological & Nuclear Sciences Monograph 13.

Ministry of Business, Innovation and Employment, 2014, New Zealand Petroleum Basins, New Zealand Petroleum & Minerals, ISSN (online): 2324-3988.

Reading H.G., 1996, Sedimentary Environments: Processes, Facies and Stratigraphy, 3rd Edition, University of Oxford, UK.

Ringrose P., and Bentley M., 2015, Reservoir Model Design – A Practitioner's Guide, Springer Science.

Strogen D.P., Kyle J. Bland, Jan R. Baur, and Peter R. King, 2012, Regional Paleogeography and Implications for Petroleum Prospectivity, Taranaki Basin,New Zealand, AAPG Search and Discovery Article #10432.

University of Canterbury Campus, 2006, A Report on Possible Government Interventions to Promote the Sustainable Development of New Zealand's Ocean Resources, http://www.mfe.govt.nz/node/6974.

Walcott R.I., 1987, Geodetic strain and the deformational history of the North Island of New Zealand during the late Cainozoic, Mathematical and Physical Sciences, A321, 163-181, Royal Society of London, London.